



Quantifying river water contributions to riparian trees along a losing river: Lessons from stable isotopes and iteration method

Yue Li^{1,2}, Ying Ma^{1,2}, Xianfang Song^{1,2}, Qian Zhang³

¹Key Laboratory of Water Cycle and Related Land Surface Processes, Institute of Geographic Sciences and
5 Natural Resources Research, Chinese Academy of Sciences, Beijing 100101, China

²University of Chinese Academy of Sciences, Beijing 100049, China

³Institute of Geographic Sciences and Natural Resources Research, Chinese Academy of Sciences, Beijing 100101,
China

Correspondence to: Ying Ma (maying@igsrr.ac.cn)

10 **Abstract.** River water plays a critical role in riparian plant water use and riparian ecosystem restoration along
losing rivers (rivers losing flow into underlying groundwater) under climate warming. How to quantify the
contributions of river water to riparian plants under different water tables and the related responses of plant water
use efficiency is a great challenge. In this study, experiments of stable isotopes ($\delta^2\text{H}$, $\delta^{18}\text{O}$ and ^{222}Rn) in different
waters and leaf $\delta^{13}\text{C}$ were conducted for riparian deep-rooted *Salix babylonica* (L.) during dry year (2019) and
15 wet year (2021) along the Chaobai River in Beijing, China. The MixSIAR model in combination with an iteration
method were proposed to quantify the proportional river water contribution (RWC) to riparian *S. babylonica* and
its correlations with the depth of water table (WTD) as well as leaf $\delta^{13}\text{C}$. Results showed that riparian *S. babylonica*
took up deep water (in 80–170 cm soil layer and groundwater) by $56.5 \pm 10.8\%$. River water that recharged
riparian deep water was an indirect water source and contributed 20.3% of water to riparian trees nearby the losing
20 river. Significantly increasing river water acquisitions (by 7.0%) but decreasing leaf $\delta^{13}\text{C}$ (by -2.0%) of riparian
trees were observed as the WTD changed from 2.7 m in 2019 to 1.7 m in 2021 ($p < 0.05$). A short residence time
(no more than 0.28 days) of groundwater indicated that there was rapid and frequent river recharge to riparian
groundwater in 2021. It was found that the RWC to riparian *S. babylonica* was negatively correlated with the
WTD but positively related to the leaf $\delta^{13}\text{C}$ in linear functions ($p = 0.000$). The rising water table would stimulate
25 riparian trees to maximize transpiration water consumptions and show a profligate water use strategy with
increasing water extraction from the losing river. This study provides critical insights into understanding the
mechanism of water cycle in Groundwater-Soil-Plant-Atmosphere Continuum, managing water resources and
riparian afforestation along losing rivers.



1 Introduction

30 Ongoing climate warming as well as groundwater overexploitation has altered precipitation regimes, river flow
and bank storage globally, further leading to widespread risks of rivers losing flow into underlying groundwater
("losing" river) and even running dry (Winter et al., 1998; Schindler and Donahue, 2006; Allen et al., 2015;
Jasechko et al., 2021). Ecological water replenishment of losing rivers and riparian revegetation have been pushed
forward worldwide to restore the river ecosystem (Smith et al., 2018; Long et al., 2020). Water replenishing to
35 losing rivers contributed 40% to bank storage and groundwater storage recovery (Long et al., 2020). However,
large-scale riparian revegetation increased the plant transpiration substantially, which in turn led to great loss of
riparian bank storage and even river flow (Moore and Owens, 2012; Dzikiti et al., 2013; Missik et al., 2019;
Mkunyana et al., 2019). Therefore, deeply understanding where and how much water riparian trees took up and
their responses to the variations in the water table could help to balance the river flow and water requirement of
40 revegetated riparian species.

The river water contribution (RWC) to riparian trees has been widely estimated using the data comparison,
graphical inference, two- or multi-source linear mixing models and Bayesian mixing models (MixSIR, SIAR,
SISUS, MixSIAR) accompanied with stable water isotopes ($\delta^2\text{H}$ and $\delta^{18}\text{O}$) (Dawson and Ehleringer, 1991;
Ehleringer and Dawson, 1992; White and Smith, 2020). Most of previous studies considered river water as a
45 separate water source to quantify the river water uptake of riparian trees (Alstad et al., 1999; Zhou et al., 2017;
White and Smith, 2020). A number of previous studies showed that the separate river water source contributed up
to 80% to riparian plant transpiration directly based on the stable isotopic signatures of different waters (Dawson
and Ehleringer, 1991; Busch et al., 1992; Alstad et al., 1999; Zhou et al., 2017; White and Smith, 2020). For
example, riparian *Liquidambar styraciflua* growing along a perennial stream took up river water by 30–35% in
50 the southern Appalachian foothills, USA (White and Smith, 2020). Alstad et al. (1999) found that riparian *Salix*
relied on rivers for approximately 80% of its water, which made it vulnerable to changes in river water and
hydrological conditions on the northeast side of Rocky Mountain National Park, Colo.

However, there was a debate on whether the river water is a potential water source for riparian trees or not
and how it became available to plants. Some studies argued that river water was not a direct potential water source
and rarely contributed to riparian trees. Dawson and Ehleringer (1991) firstly discovered that mature streamside
55 trees growing in or next to a perennial river did not use river water but depended on waters from deeper strata.



This finding has also been proven in riparian phreatophytic trees (*Populus fremontii* and *Salix gooddingii*) and riparian deep-rooted tree species (Busch et al., 1992; Bowling et al., 2017; Wang et al., 2019a). Even under shallow groundwater with high salinity, no river water was directly absorbed by riparian *Eucalyptus coolabah* alongside
60 an ephemeral arid zone river in Australia (Costelloe et al., 2008). Other studies claimed that river water merging into deep riparian soils and groundwater could be indirectly utilized by riparian trees under shallow water table conditions (Mensforth et al., 1994; Wang et al., 2019b). It remained unclear that how much river water exactly contributed to riparian trees nearby a losing river. This might lead to inaccurate estimations when river water could not be directly accessed by lateral roots of riparian trees growing at a certain distance away from the riverbank
65 (Mensforth et al., 1994; Thorburn and Walker, 1994). How to separate and quantify the indirect contributions of river water to riparian trees nearby losing rivers is a great challenge.

The RWC could substantially affect the leaf-level water use efficiency (WUE) and healthy growth of riparian trees. The WUE is a key characteristic of plant water use, which can be defined as the ratio of photosynthetic rate to transpiration rate. Since leaf $\delta^{13}\text{C}$ values are positively related to WUE, the leaf $\delta^{13}\text{C}$ has been widely used as
70 an indicator of WUE (Farquhar et al., 1989). Thorburn and Walker (1994) found that the riparian *Eucalyptus camaldulensis* beside the ephemeral stream had higher WUE with more frequent access to river water based on the leaf $\delta^{13}\text{C}$ measurements. Nevertheless, Sun et al. (2008) observed that the river water availability had little effect on WUE because there was no significant difference in WUE between riparian *Pinus massoniana* and non-riparian *Pinus quercus*. Several previous studies reported that the WUE of riparian trees varied with the fluctuation
75 of water table depth (WTD) in the riparian zone due to changing river flow (Horton and Clark, 2001; Liu et al., 2017; Xia et al., 2018). For example, Horton and Clark (2001) showed that the WUE of riparian *Salix gooddingii* and *Populus fremontii* increased with increasing WTD, and riparian *Tamarix chinensis* had significantly higher WUE under fluctuated deep WTD in dry year than those under constant shallow WTD in wet year. In comparison, the WUE of riparian species decreased significantly along a gradient of increasing WTD (from 0.5 m to 12 m) in
80 the middle reaches of Heihe River Basin, China (Liu et al., 2017). However, little attention has been paid to quantifying the relationships between the RWCs to riparian trees and WUE as well as WTD.

The aim of this study was to clarify the effects of river water on water use of riparian trees along a gradient of WTD. Focusing on a losing river in Beijing, China, the objectives of this study were: (1) to propose an iteration method together with water stable isotopes ($\delta^2\text{H}$ and $\delta^{18}\text{O}$) to quantify the RWCs; (2) to determine the proportional



85 contributions of river water to riparian trees at different distances away from the riverbank; (3) to identify the relationships between the RWCs to riparian trees and WUE (indicated by leaf $\delta^{13}\text{C}$ values) as well as WTD. These results will provide critical insights into plantation management, bank storage conservation and healthy ecosystem enhancement for losing rivers.

2 Materials and methods

90 2.1 Study area

The study area was in the reaches of the Chaobai River, located in Shunyi district, Beijing, China ($40^{\circ}07'30''\text{N}$, $116^{\circ}40'37''\text{E}$) (Fig. 1). The temperate continental sub-humid monsoon climate prevails in this area, with an annual mean temperature and evaporation of 11.5°C and 1175 mm , respectively. Due to continuous drought and groundwater overexploitation, the Chaobai River dried up during 1999 to 2007 and the riparian ecosystem degraded seriously. The ecological water has been supplied to restore this dry river since 2007, and more than 33 km^2 of the riparian zone has been recovered with different tree species by 2020. The *S. babylonica* was one of the most widely planted species alongside the Chaobai River. Three plots at distances of 5 m (D05), 20 m (D20), and 45 m (D45) away from the riverbank were selected for field measurements and sample collection (Fig. 1).

2.2 Field measurements

100 The field measurements were conducted during April to November in 2019 and 2021, with no field observation in 2020 due to the COVID-19. The daily precipitation data from 1961 to 2021 in the Shunyi district was collected from the China Meteorological Data Service Centre (<http://data.cma.cn/en>). The groundwater levels in each plot were recorded monthly in 2019 and 2021 via the pressure stage gauge (HOH-S-Y, King Water Co Ltd., Beijing, China) installed in the groundwater monitoring well. The river water level was recorded using a water gauge at the same time with the observation of groundwater levels. The average total precipitation during April to November between 1961 and 2021 is 532.8 mm (Fig. 2a). The observation period in 2021 was wet with total precipitation of 802.5 mm , which was 1.8 times of that in dry year of 2019 (445.6 mm) (Fig. 2b and c). The river water level fluctuated at $27.9\text{--}28.9\text{ m}$ in 2019 and $27.3\text{--}29.7\text{ m}$ in 2021 (Fig. 3). The mean WTD in three plots in 2019 ($2.7 \pm 0.3\text{ m}$) was significantly larger than that in 2021 ($1.7 \pm 0.5\text{ m}$) ($p < 0.05$). The WTD decreased with increasing distances from the riverbank in both 2019 and 2021.



2.3 Sample collection and isotopic analyses

Twelve sampling campaigns on May 5, Jun 14, Jul 26, Aug 15, Sep 26, Nov 5 in 2019 and Apr 24, May 25, Jun 26, July 15, Sep 1, Nov 5 in 2021 were conducted to collect groundwater, precipitation, river water, soil, stem, and leaf samples. Groundwater in each plot was sampled by a sucking pump from the monitoring well, and a hydrophore was used to collect the nearby river water. A total of 135 precipitation samples were collected in the observation period via a device consisting of a funnel, a polyethylene bottle and a ping-pong ball. All precipitation, groundwater, and river water samples were stored at 4 °C in the refrigerator until water isotope ($\delta^2\text{H}$ and $\delta^{18}\text{O}$) analysis. The groundwater and river water were also collected with brown bottles to measure ^{222}Rn concentration in the study area.

Three riparian *S. babylonica* trees (with mean diameter of 28.6 ± 4.4 cm at breast height) growing in three plots were chosen on each sampling campaign for $\delta^2\text{H}$ and $\delta^{18}\text{O}$ measurements in stem water as well as $\delta^{13}\text{C}$ analysis in plant leaves. Several suberized stems were firstly cut from riparian *S. babylonica*, removed the bark and phloem, and then stored at -10 °C until water isotope analysis. The mature leaves were sampled from the collected stems, oven-dried at 65 °C for 72 h, then grinded and passed through a 0.15 mm sieve to analyze leaf $\delta^{13}\text{C}$.

Soils at depths of 0–5, 5–10, 10–20, 20–30, 40–60, 60–80, 90–110, 150–170, 190–210, 250–270, and 280–300 cm nearby the selected *S. babylonica* trees were sampled by a power auger (CHPD78, Christie Engineering Company, Sydney, Australia). One part of each soil sample was put into a 12-ml glass vial and stored at -10 °C for water stable isotope analysis, and the other part was packed into an aluminum box for gravimetric soil water content (SWC) measurement via the oven-dry method.

The automatic cryogenic vacuum distillation system (LI-2100, LICA, Beijing, China) was used to extract water in stem and soil samples, which generally ran for at least 2.5 h and kept the efficiency of water extraction more than 99% to ensure no isotopic fractionation. The $\delta^2\text{H}$ and $\delta^{18}\text{O}$ in soil water, river water, groundwater, and precipitation were analyzed through an isotopic ratio infrared spectroscopy system (IRIS) (DLT-100, Los Gatos Research, Mountain View, USA) (Li et al., 2021). The Isotope Ratio Mass Spectrometry system (IRMS) (MAT253, Thermo Fisher Scientific, Bremen, Germany) which could prevent from organic pollution of plants was used to measure $\delta^2\text{H}$ and $\delta^{18}\text{O}$ in stem water as well as leaf $\delta^{13}\text{C}$ value. There was the same measurement accuracy of $\pm 1\%$ for $\delta^2\text{H}$ and $\pm 0.1\%$ for $\delta^{18}\text{O}$ between the IRIS and IRMS systems. The Vienna Standard Mean Ocean Water



(VSMOW) was used to calibrate and normalize the $\delta^2\text{H}$ and $\delta^{18}\text{O}$ measurements in different waters, while the
140 Vienna Pee Dee Belemnite (V-PDB) was used for calibrating leaf $\delta^{13}\text{C}$ values.

The ^{222}Rn concentration in the groundwater and river water samples (C_{Water} , Bq/l) was determined based on
the ^{222}Rn concentration measured by a ^{222}Rn monitor (Alpha GUARD PQ2000 PRO, Bertin Instruments, Germany)
(C_{Air} , Bq/m³). 100 ml of the water sample was slowly poured into the air-tight glass bottles and then purged with
air in a closed gas cycle system. The C_{Air} was recorded at 10-minute intervals, and more than four intervals were
145 conducted to ensure that the ^{222}Rn concentration in the measuring set-up before sampling (background) (C_{System} ,
Bq/m³) was less than 80 Bq/m³. The measurement range of C_{Air} was 2–2,000,000 Bq/m³ with a measurement
precision of 3%. The C_{Water} can be calculated as:

$$C_{\text{Water}} = \frac{C_{\text{Air}} \times \left(\frac{V_{\text{System}} - V_{\text{Sample}}}{V_{\text{Sample}}} + k \right) - C_{\text{System}}}{1000} \quad (1)$$

where V_{System} is the interior volume of the measuring set-up (ml), which is 1122 ml in this study. V_{Sample} is the
150 volume of water sample (ml). k is the ^{222}Rn distribution coefficient of water/air (–), which can be set as 0.26 within
the specified temperature range around a mean room temperature of 20 °C.

2.4 Determination of RWC to riparian trees

Riparian trees at a certain distance away from the riverbank rarely used river water directly, as their lateral roots
could not reach the river (Mensforth et al., 1994; Thorburn and Walker, 1994). Nevertheless, riparian trees could
155 continuously absorb river water that merged into riparian deep water (including groundwater and deep soil water
within the capillary fringe) when their deep roots tapped into the water table. In this study, water stable isotopes
($\delta^2\text{H}$ and $\delta^{18}\text{O}$) integrated with the MixSIAR model and an iteration method were proposed to identify the original
(before and during the observation period) contributions of river water that merged into riparian deep water to
riparian *S. babylonica* trees (Fig. 4). Firstly, the root water uptake patterns were determined via $\delta^2\text{H}$ and $\delta^{18}\text{O}$ in
160 different waters and the MixSIAR model, without considering river water as a direct water source for riparian
trees. Secondly, the proportional contributions of river water to riparian deep water were figured out by the
MixSIAR model and water isotopes. Finally, the proposed iteration method was used to quantify the proportions
of the RWC to riparian trees (Fig. 4).



2.4.1 Quantifying direct water source contributions to riparian trees

165 In this study, soil water at different depths, which was mixed proportionally with precipitation, old soil water, or
even river water and groundwater, was taken up by riparian *S. babylonica* directly. Groundwater also could be
regarded as a relatively stable water source for phreatophyte riparian trees (Dawson and Ehleringer, 1991; Busch
et al., 1992). In terms of seasonal variations in the SWC, water isotopes and WTD, four soil layers (0–30, 30–80,
80–170, and 170–300 cm) were divided to identify the main root water uptake depth of riparian trees in the three
170 plots (Figs. 2, 3 and S1). As the isotopic composition of soil water in 170–300 cm layer was similar to that of
groundwater, they were considered to be one water source (groundwater). Therefore, soil water in 0–30, 30–80,
80–170 cm layers, and groundwater were determined as the direct water sources for riparian *S. babylonica*. Due
to the $\delta^2\text{H}$ offset of stem water from its potential sources, the measured stem water $\delta^2\text{H}$ values were corrected via
the potential water source line proposed by Li et al. (2021). The raw $\delta^{18}\text{O}$ and corrected $\delta^2\text{H}$ in stem water were
175 set as the mixture data in the MixSIAR model to quantify the direct water source contributions to riparian *S.*
babylonica. The parameter settings of the MixSIAR model have been described in detail by Stock and Semmens
(2013) and Li et al. (2021). The contributions of riparian deep soil water in 80–170 cm layer to riparian trees (P_s)
and the groundwater contributions to riparian trees (P_g) could be determined in particular to evaluate the RWCs
to riparian trees.

180 2.4.2 Identifying water sources for deep soil water and groundwater

Riparian deep soil water and groundwater could be continuously recharged by river water when the groundwater
levels lied below the riverbeds (i.e., losing rivers). The MixSIAR model in conjunction with water isotopes ($\delta^2\text{H}$
and $\delta^{18}\text{O}$) were applied to quantify the RWCs to riparian deep water. As shown in Fig. S2a, the potential water
sources of riparian deep soil water in 80–170 cm layer at current sampling time (t) included the in-situ soil water
185 in this layer at previous sampling time (t-1), soil water in 0–80 cm layer at t-1, river water between t-1 and t,
precipitation between t-1 and t, and groundwater between t-1 and t. The potential water sources for riparian
groundwater at t were considered as the in-situ groundwater at t-1, soil water in 0–170 cm layer at t-1, river water
between t-1 and t, and precipitation between t-1 and t (Fig. S2b). The $\delta^2\text{H}$ and $\delta^{18}\text{O}$ in riparian deep water (deep
soil water in 80–170 cm layer or groundwater) at t were set as the mixture data in the MixSIAR model, while the
190 water isotopes of their potential sources were considered as the source data.



In this study, the average residence time (T_{res}) of groundwater recharged from the river to the underlying aquifer and/or riverbank was also identified based on the ^{222}Rn isotopes, which was described as follows:

$$T_{res} = \frac{1}{\lambda} \times \ln \left(\frac{C_e - C_r}{C_e - C_g} \right) \quad (2)$$

where λ represents the decay coefficient (0.181 d^{-1}). C_e represents the ^{222}Rn concentration when the equilibrium between radon production and decay is reached (7400 Bq/m^3 in this study); C_r represents the ^{222}Rn concentration of river water (Bq/m^3); C_g represents the ^{222}Rn concentration of groundwater (Bq/m^3).

2.4.3 An iteration method to determine RWCs to riparian trees

The proportional contributions of the river water between t-1 and t to riparian trees could be quantified when riparian deep-water contributions to trees and the RWCs to riparian deep water were both figured out. It was noted that the riparian in-situ deep water (i.e., in-situ 80–170 cm soil water and in-situ groundwater) were also merged by old river water before t-1. In this study, the contributions of old river water before t-1 to riparian in-situ deep water were assumed to be consistent with those proportions of river water between t-1 and t to riparian in-situ deep water (i.e., “ s_r ” and “ g_r ”). An iteration method was proposed to quantify the original RWC to *S. babylonica* trees nearby the losing rivers, which was described as follows:

$$\begin{aligned} \text{RWC} &= P_s * S_r + P_g * G_r \\ &= P_s * (s_r + s_r^0) + P_g * (g_r + g_r^0) \\ &= P_s * (s_r + s_r * s_s + s_r * s_s^2 + s_g * g_r + s_g * g_r * g_g + s_g * g_r * g_g^2) + P_g * (g_r + g_r * g_g + g_r * g_g^2) \\ &= P_s * s_r * (1 + s_s + s_s^2) + P_s * s_g * g_r * (1 + g_g + g_g^2) + P_g * g_r * (1 + g_g + g_g^2) \\ &= (P_s * s_r + P_g * g_r + P_s * s_g * g_r) + (P_s * s_r * s_s + P_g * g_r * g_g + P_s * g_r * s_g * g_g) + (P_s * s_r * s_s^2 + P_g * g_r * g_g^2 + P_s * s_g * g_r * g_g^2) \quad (3) \end{aligned}$$

where S_r and G_r represent original (before and during the observation period) RWCs to riparian deep soil water in 80–170 cm layer and groundwater, respectively. The s_r^0 and g_r^0 represent the proportional contributions of the old river water (before t-1) to riparian deep soil water in 80–170 cm layer and groundwater, respectively. The s_s , s_r , and s_g represent the proportional contributions of in-situ soil water in 80–170 cm layer at t-1, river water during t-1 to t, and groundwater during t-1 to t for riparian deep soil water in 80–170 cm layer at t, respectively. The g_g and g_r represent the proportional contributions of in-situ groundwater at t-1 and river water from t-1 to t for riparian groundwater at t, respectively. The expression of “ $P_s * s_r + P_g * g_r + P_s * s_g * g_r$ ” in Equation (3) was proposed to determine the current river water (between t-1 and t) contributions to riparian trees. The second iteration ($P_s * s_r * s_s$,



+ $P_g * g_r * g_g + P_s * g_r * s_g * g_g$) and the third iteration ($P_s * s_r * s_s^2 + P_g * g_r * g_g^2 + P_s * s_g * g_r * g_g^2$) were used to quantify the proportional contributions of old river water before t-1 that merged into riparian in-situ deep water to trees (Fig. 4). Only three iterations were applied in this study, because the differences between the RWCs in the third iteration and the next iteration were less than 0.1%. Using this proposed iteration method, the complete proportions of old and current river water recharged riparian deep water could be estimated.

2.5 Data analysis

The statistic differences in WTDs, SWC, $\delta^2\text{H}$ and $\delta^{18}\text{O}$ in different water bodies, ^{222}Rn concentration of river water and groundwater, potential water source contributions, and leaf $\delta^{13}\text{C}$ values among the three plots in 2019 and 2021 were analyzed by One-way analysis of variance incorporating with Kolmogorov-Smirnov, Levene's and post-hoc Tukey's tests ($p < 0.05$). The relationships between the WTD, leaf $\delta^{13}\text{C}$ values and RWCs to riparian trees were determined by the regression analysis method. The statistical analysis was performed in the Excel (v2016) as well as SPSS (24.0, Inc., Chicago, IL, USA).

230 3 Results

3.1 Water uptake patterns of riparian trees

It was evident in Fig. 5 that the $\delta^2\text{H}$ and $\delta^{18}\text{O}$ in precipitation was significantly more depleted in 2021 ($-52.9 \pm 30.2\text{‰}$ for $\delta^2\text{H}$ and $-8.1 \pm 3.8\text{‰}$ for $\delta^{18}\text{O}$) than those in 2019 ($-29.2 \pm 18.8\text{‰}$ for $\delta^2\text{H}$ and $-4.1 \pm 3.0\text{‰}$ for $\delta^{18}\text{O}$) ($p < 0.05$). The significantly larger slope of the Local Meteoric Water Line in 2021 (7.8) with respect to that in 2019 (5.5) also suggested more depleted precipitation isotopes in 2021 ($p < 0.05$). Significantly higher SWC was observed in 2021 compared with that in 2019 ($p < 0.05$) (Fig. S1). The SWC of all four soil layers at D45 was significantly lower than that at D05 and D20 in 2021 ($p < 0.05$), while no pronounced difference in SWC of 0–30 cm layer was observed among three plots in 2019 ($p > 0.05$) (Fig. S1). The $\delta^2\text{H}$ and $\delta^{18}\text{O}$ in soil water in 0–30 cm layer in 2021 were significantly more depleted and more variable than those in 2019 ($p < 0.05$) (Fig. 5). Nevertheless, there were slightly enriched water isotopes in 30–170 cm soil layer in 2021 compared with those in 2019. No significant difference in the isotopic compositions of soil water below 170 cm depth and groundwater was observed between 2019 and 2021 ($p > 0.05$). As shown in Fig. 5, the isotopes in groundwater were significantly more depleted than those in river water in both years ($p < 0.05$). The $\delta^2\text{H}$ and $\delta^{18}\text{O}$ in stem water



during the observation periods in 2019 and 2021 were not significantly different ($p > 0.05$), but they were gradually
245 depleted with the increasing distances in riparian zone.

The contributions of superficial soil water (above 30 cm depth) to riparian trees in 2019 ($20.1 \pm 9.7\%$) were
similar to those in 2021 ($19.0 \pm 10.5\%$). As shown in Fig. 6, no significant difference in the soil water contributions
to riparian *S. babylonica* was also observed in 30–80 cm layer between the two years ($p > 0.05$). The *S. babylonica*
tree species principally relied on riparian deep water below 80 cm depth in both 2019 (55.9%) and 2021 (57.1%).
250 The soil water contributions in 80–170 cm layer to riparian trees reduced with the distance away from the
riverbank in both years, whereas the groundwater contributions increased from D05 to D45 in both 2019 (from
27.6% to 32.1%) and 2021 (from 17.0% to 32.2%) (Fig. 6). It was found that the groundwater contributions
increased evidently from April to July but they plummeted and reached minimum in September in 2021.

3.2 Water source contributions to riparian deep soil water and groundwater

255 Significant seasonal and interannual variations of different water source contributions to riparian deep soil water
in 80–170 cm layer were found during the observation periods in the study area ($p < 0.05$). Riparian deep soil
water was primarily recharged by the in-situ soil water (mean of 33.1%) and groundwater capillary rise (mean of
25.3%) in 2019 (Fig. 7). In comparison, the in-situ soil water (mean of 23.9%), groundwater capillary rise (mean
of 24.6%), and river water (mean of 24.4%) contributed evenly to riparian deep soil water in 2021. The in-situ
260 soil water contribution in 2019 was significantly higher than that in 2021 ($p < 0.05$). However, the river water
contributed less to riparian deep soil water in 2019 (mean of 15.7) compared with 2021 ($p < 0.05$). The RWC to
riparian deep water was lowest in August in 2019 ($11.3 \pm 4.5\%$) but in June in 2021 ($13.6 \pm 3.8\%$). The in-situ
soil water contributions showed a significant increase with distance away from the riverbank, while the RWCs
decreased from D05 to D45 in both years ($p < 0.05$) (Fig. 7).

265 There were significant differences in interannual and seasonal water source contributions to riparian
groundwater in three plots in dry 2019 and wet 2021 ($p < 0.05$). The in-situ groundwater was the main source of
riparian groundwater in both years (Fig. 8), but its contribution was significantly higher in 2019 (mean of $56.0 \pm$
 11.2%) than that in 2021 ($37.1 \pm 16.7\%$). The riparian groundwater was recharged by river water with mean of
 $28.1 \pm 12.1\%$ during the observation period. There was a significantly higher RWC to riparian groundwater in
270 2021 (mean of $35.1 \pm 11.9\%$) than that in 2019 (mean of $21.1 \pm 7.2\%$) ($p < 0.05$). The lowest RWC ($13.0 \pm 1.2\%$)
showed in August with the lowest water table of 3.1 m in 2019, whereas river water contributed most ($47.1 \pm$



13.2%) to riparian groundwater in July with higher water table of 1.8 m in 2021. The in-situ groundwater contributions increased with the distances during the observation periods, while RWCs decreased significantly from D05 to D45 ($p < 0.05$) (Fig. 8). As shown in Table 2, there was a significant increase of ^{222}Rn activities in
275 groundwater from D05 ($494.5 \pm 107.5 \text{ Bq/m}^3$) to D45 ($787.4 \pm 153.2 \text{ Bq/m}^3$) ($p < 0.05$). The T_{res} of groundwater that recharged by river to the underlying aquifer and/or riverbank increased from D05 (-0.09 ± 0.09 days) to D45 (0.15 ± 0.13 days) (Table 2). These also indicated that the river recharge to riparian deep strata was rapid and frequent, particularly more evident in the plots closer to the riverbank.

3.3 Seasonal variations in RWC to riparian trees

280 Significant differences in the seasonal RWCs to riparian *S. babylonica* were found between dry 2019 and wet 2021 ($p < 0.05$). As shown in Fig. 9, the proportional contributions of river water to *S. babylonica* were significantly more in 2021 (mean of $23.8 \pm 7.8\%$) than those in 2019 (mean of $16.8 \pm 4.7\%$) ($p < 0.05$). In particular, riparian *S. babylonica* took up significantly more river water in July ($35.2 \pm 7.0\%$) and November ($29.0 \pm 5.0\%$) in 2021 than that in July ($15.4 \pm 1.7\%$) and November ($14.8 \pm 1.6\%$) in 2019 ($p < 0.001$). The least absorption of
285 river water for *S. babylonica* was $17.7 \pm 2.7\%$ in 2021 (in September), which was larger than that of $13.2 \pm 1.9\%$ in 2019 (in August). The most absorption of river water occurring in July in 2021 was also larger than that of $24.2 \pm 3.0\%$ observed in June in 2019.

The water uptake of river water by riparian *S. babylonica* was significantly different among the three plots in 2019 and 2021 ($p < 0.05$). The RWC to riparian trees decreased significantly by 6.9% from D05 (20.0%) to
290 D45 (13.1%) in 2019 ($p < 0.05$), whereas the corresponding value reduced little by 2.6% (from 25.3% to 22.72%) along the distances in 2021 ($p > 0.05$).

3.4 Relationships of leaf $\delta^{13}\text{C}$ with RWCs to riparian trees and WTD

The seasonal leaf $\delta^{13}\text{C}$ of riparian *S. babylonica* in three plots varied significantly in 2019 and 2021 ($p < 0.05$). The leaf $\delta^{13}\text{C}$ in 2019 ($-27.7 \pm 1.0 \text{ ‰}$) was remarkably larger than that in 2021 ($-29.7 \pm 0.7 \text{ ‰}$) ($p < 0.05$) (Table
295 1). There was a significantly increase of leaf $\delta^{13}\text{C}$ from D05 (-28.8‰) to D45 (-27.0‰) in 2019 ($p < 0.05$), while no significant difference in leaf $\delta^{13}\text{C}$ was observed among different distances in 2021 ($p > 0.05$). The smallest leaf $\delta^{13}\text{C}$ value of riparian trees showed on Aug 15 in 2019 and Jul 14 in 2021, before when intense rainfall occurred.

There was a significantly negative relationship between the RWCs to riparian trees and the WTD (Fig. 10a). The leaf $\delta^{13}\text{C}$ was found to be negatively correlated with the RWCs but positively related to the WTD in linear



300 functions ($p < 0.001$) (Fig. 10b and c). These indicated that deeper WTD (2.7 ± 0.3 m) and less RWCs to riparian
S. babylonica resulted in higher leaf-level WUE in dry year of 2019. In comparison, the riparian *S. babylonica*
under relatively shallower WTD (1.7 ± 0.5 m) led to greater RWCs but smaller leaf-level WUE in 2021. It seemed
that the riparian *S. babylonica* could consume the least amount of river water for transpiration to achieve the
maximum WUE when the WTD was 4.0 m.

305 **4 Discussion**

4.1 River recharge to riparian deep soil water and groundwater

This study quantified the RWCs to riparian deep soil water within the capillary fringe and groundwater nearby a
losing river. Approximately one third of the riparian groundwater was recharged by river water, while 46.5% of
riparian groundwater was not exchanged with river water or other water sources (Fig. 8). A short residence time
310 (no more than 0.28 days) of groundwater recharged by river water in 2021 indicated that there were rapid and
frequent interactions between river water and riparian groundwater (Table 2). These contradictions might be due
to that the seepage of river water exchanged with mobile groundwater quickly but not mixing with water held
tightly in the soil pores (Brooks et al., 2010; Evaristo et al., 2015; Allen et al., 2019). It was consistent with
previous studies that the lateral seepage of river water or rising water table could briefly saturate riparian soils but
315 not replace/flush immobile waters or isotopically homogenize different water pools (Sprengr et al., 2019).

There was a significant decline of water table (0.8 m) between June and August in 2019, while the water
table increased by 1.3 m from June to November in 2021. Changes in water tables significantly affected the
interactions between riparian deep water and river water. This study confirmed that the rising water tables
stimulated riparian deep water to exchange with river water. The river water contributed significantly more to
320 riparian deep water in wet 2021 with shallower WTD of 1.7 m than that in dry 2019 with deeper WTD of 2.7 m
(Figs. 7 and 8). It agreed well with the report of Wang et al. (2021) that the amount of surface water recharge to
riparian groundwater increased with reducing WTD (ranging from 16.3 m to 2.6 m) in Baiyangdian wetland,
China. The impacts of river water on riparian deep water weakened significantly with the increase of distance
from the river. It could be inferred from the significantly declining RWCs to riparian deep water and increasing
325 residence time of groundwater along the gradient of distance ($p < 0.05$) (Figs. 7 and 8; Table 2). A number of
previous studies also indicated that the declining water table with distance resulted in weakening hydraulic



connection between river water and riparian groundwater (Stellato et al., 2013).

4.2 The roles of river water in riparian tree water uptake

This study identified that deep-rooted riparian trees nearby a losing river used a smaller proportion of river water
330 (less than 25%), even though the water uptake from deep soils and groundwater recharged by river water were
considered (Fig. 9). This finding was similar to the results reported on riparian trees nearby the perennial stream
(Busch et al., 1992; Thorburn and Walker, 1994). It underlined that other water sources rather than river water
played dominant roles in riparian tree water uptake. Global studies also concluded that 89% of plant transpiration
relied on precipitation during the growing season or that stored in the substrates from past season (Miguez-Macho
335 and Fan, 2021).

As the outer projected edge of canopy were out of reach of river, the lateral roots of riparian trees further
than 5 m away from the riverbank could not directly absorb river water (Busch et al., 1992; Thorburn and Walker,
1994). The RWC to riparian trees mainly depended on the river water recharge to deep soil water and groundwater
(less than 30%). The river water exchanged rapidly and frequently with riparian mobile deep soil
340 water/groundwater, but rarely with bound water in fine pores (Brooks et al., 2010; Evaristo et al., 2015; Allen et
al., 2019; Sprenger et al., 2019). Nevertheless, the riparian trees predominantly extended roots into fine pores to
take up bound water (Evaristo et al., 2015; Maxwell and Condon, 2016; Evaristo et al., 2019). The mobile deep
soil water/groundwater was alternative water source for riparian trees especially under drought conditions. These
discrepancies between fast-moving river water seepage and immobile water for plant water uptake probably led
345 to the small contribution of river water to riparian trees.

The temporal and spatial variations in the RWCs were significantly affected by various water tables in this
study. Shallower water table could increase the river water recharge to riparian deep water which riparian trees
mainly relied on. It was evident that riparian deep-rooted *S. babylonica* absorbed significantly more river water
in 2021 with 1 m shallower WTD than that in 2019 (Fig. 9). The decreasing RWCs along the gradient of distance
350 in both dry and wet years also confirmed that the water table decline could make riparian phreatophyte trees less
dependent on river water (Zhou et al., 2017). In contrast to the findings in this study, riparian dimorphic *G biloba*
shifted from shallow soil layer to deeper soil layer with significantly increasing absorption of river water when
the water table declined more than 1 m (Qian et al., 2017). This indicated that riparian dimorphic trees could
increase the proportions of river water absorption in response to the water table decline, while the RWCs to



355 riparian phreatophytic/deep-rooted trees decreased with the water table decline.

4.3 Responses of WUE to riparian tree uptake of river water and WTD

There was a balance and coordination between the soil water availability and river water absorption as well as leaf-level WUE of riparian trees, because obvious differences in the RWCs and leaf $\delta^{13}\text{C}$ values were found in three plots between dry and wet years in this study (Fig. 9 and Table 2). The riparian *S. babylonica* grew more
360 reliance on river water and the WUE significantly decreased with frequent precipitation and rising groundwater level in wet year ($p < 0.05$) (Figs. 9, 10a and 10b). This might be ascribed to that the high-water availability could stimulate riparian trees to maximize their transpiration rate and show a profligate water use strategy with growing water extraction from river. It agreed well with previous studies that woody plants showed profligate water-use patterns and relatively lower WUE in rainy season, whereas they had higher WUE and conservative water-use
365 patterns as the soil water availability decreased in dry season (Horton and Clark, 2001; Cao et al., 2020). However, the profligate water use strategy of riparian trees could result in overconsumption of river flow, which indicated that rising water tables would not be recommended in this shallow WTD area. These leaf-level ecophysiological characteristics (i.e., water use efficiency and transpiration rate) of riparian trees responded quickly to the changing water tables.

370 It was evident that the WTD played a critical role in river water acquisition and WUE of riparian trees nearby losing rivers (Mensforth et al., 1994; Horton and Clark, 2001; Qian et al., 2017; Zhou et al., 2017). This study indicated that the increasing WTD linearly reduced the reliance of riparian trees on river water sources, mainly due to the diminishing water exchanges between river water and riparian groundwater with the water table decline (Figs. 7, 8 and 10a). In comparison, the declining water table proportionally increased the leaf $\delta^{13}\text{C}$ of riparian *S.*
375 *babylonica* (Fig. 10b), which was consistent with previous studies that an exponential growth function existed between the leaf $\delta^{13}\text{C}$ of riparian *Salix gooddingii* and WTD ($\delta^{13}\text{C} = 2.76 - 24.78 \times \exp^{-0.02\text{WTD}}$, $0 < \text{WTD} < 10$ m) (Horton and Clark, 2001). In this study, the 4 m of WTD seemed to be optimal to coordinate the riparian plant-water relations, when the riparian *S. babylonica* consumed the least amount of river water for transpiration and showed highest WUE. This benefited for balancing the relationship between the riparian tree growth and river
380 flow reservation. Nevertheless, there were some controversial views that the WUE of plant species firstly increased and then decreased with increasing WTD, and the maximum WUE occurred when WTD was 1.44 m (Xia et al., 2018) or 6 m (Antunes et al., 2018). The knee point of WTD was not observed in this study, suggesting



that further investigations should be conducted under deeper water tables (> 4 m) to quantify the relationships among water tables, WUE and RWCs to riparian trees.

385 **4.4 Further scopes**

Riparian trees could only indirectly absorb river water that merges into riparian deep water when they grow at a certain distance away from the riverbank. Inaccurate estimation of the RWCs to riparian trees nearby the losing rivers would be resulted once river water is identified as a separate source, but it can be resolved by the newly developed iteration method in this study. When river water merging into riparian deep water is utilized by riparian trees, the iteration method could accurately separate and quantify the indirect contributions of river water to riparian trees. The iteration method has been proven to be available for quantifying the RWCs to those riparian trees growing under shallow WTD conditions along the losing river in this research. However, it still requires further improvements under more cases with deeper WTDs. Moreover, the proportions of old river water merging into riparian deep water before the initial time need more investigation by collecting prior water samples. It is evident that quantifying the relationships among the RWCs to riparian tree species, WTD and WUE provides critical insights into coordinating and balancing the river water conservation and riparian plant transpiration in losing rivers.

5 Conclusions

This study presented a new iteration method together with stable water isotopes ($\delta^2\text{H}$ and $\delta^{18}\text{O}$) and the MixSIAR model to separate and quantify the indirect contributions of river water to riparian *S. babylonica* in dry 2019 and wet 2021 along a losing river in Beijing, China. The infiltrating river water could quickly exchange with mobile water (with a proportion of 24.1%) but not mixing with waters held tightly in the fine pores. Riparian trees nearby a perennial stream generally extended roots into fine pores to access to slow-moving water sources, only taking up a small amount of fast-moving river water (20.3%). More river water could be absorbed and lower leaf $\delta^{13}\text{C}$ was resulted in wet year when the WTD was 1 m shallower than that in dry year. The RWCs to riparian trees decreased along the distance away from the riverbank. Increasing WTD linearly reduced the reliance of riparian trees on river water sources ($p < 0.001$). It was found that leaf $\delta^{13}\text{C}$ showed a negatively correlation with the RWCs but was positively related to the WTD in linear functions ($p < 0.001$). These suggested that rising water table would promote riparian trees to show a profligate water use strategy and increase the river water acquisitions. The



410 maximum WTD of 4 m seemed to be optimal for riparian plant-water relations, maintaining highest water use
efficiency and minimizing the plant transpiration. This study provides valuable insights into riparian afforestation
related to water use and healthy riparian ecosystem enhancement.

Data availability: The data that support the findings of this study are available from the corresponding author
415 upon request.

Author contributions: YL: Investigation, Methodology, Formal analysis, Writing - original draft, Writing -
review & editing; YM: Methodology, Formal analysis, Conceptualization, Writing - review & editing; XFS:
Supervision, Writing - review & editing, Project administration; QZ: Methodology.

420

Competing interests: The authors declare that they have no conflict of interest.

Acknowledgements: This work was supported by the National Natural Science Foundation of China
(41730749) and the National Key R&D Program of China (2021YFC3201203). Sincere thanks go to Xue Zhang,
425 Yiran Li, Lihu Yang and Binghua Li for their assistance in experiments.

Reference

- Allen, C. D., Breshears, D. D., and McDowell, N. G.: On underestimation of global vulnerability to tree mortality
and forest die-off from hotter drought in the Anthropocene. *Ecosphere*. 6, doi:10.1890/ES15-00203.1, 2015.
- 430 Allen, S. T., Kirchner, J. W., Braun, S., Siegwolf, R. T. W., and Goldsmith, G. R.: Seasonal origins of soil water
used by trees. *Hydrology and Earth System Sciences*. 23, 1199-1210, 2019.
- Alstad, K. P., Welker, J. M., Williams, S. A., and Trlica, M. J.: Carbon and water relations of *Salix monticola* in
response to winter browsing and changes in surface water hydrology: an isotopic study using delta C-13
and delta O-18. *Oecologia*. 120, 375-385, 1999.
- 435 Antunes, C., Barradas, M. C. D., Zunzunegui, M., Vieira, S., Pereira, A., Anjos, A., Correia, O., Pereira, M. J.,
and Maguas, C.: Contrasting plant water-use responses to groundwater depth in coastal dune ecosystems.



- Functional Ecology. 32, 1931-1943, 2018.
- Bowling, D. R., Schulze, E. S., and Hall, S. J.: Revisiting streamside trees that do not use stream water: can the two water worlds hypothesis and snowpack isotopic effects explain a missing water source? *Ecohydrology*. 10, 1-12, doi:10.1002/eco.1771, 2017.
- 440 Brooks, J. R., Barnard, H. R., Coulombe, R., and McDonnell, J. J.: Ecohydrologic separation of water between trees and streams in a Mediterranean climate. *Nature Geoscience*. 3, 100-104, 2010.
- Busch, D. E., Ingraham, N. L., and Smith, S. D.: Water uptake in woody riparian phreatophytes of the Southwestern United States: A stable isotope study. *Ecological Applications*. 2, 450-459, 1992.
- 445 Cao, M., Wu, C., Liu, J. C., and Jiang, Y. J.: Increasing leaf $\delta^{13}\text{C}$ values of woody plants in response to water stress induced by tunnel excavation in a karst trough valley: Implication for improving water-use efficiency. *Journal of Hydrology*. 586, 124895, doi:10.1016/j.jhydrol.2020.124895, 2020.
- Costelloe, J. F., Payne, E., Woodrow, I. E., Irvine, E. C., Western, A. W., and Leaney, F. W.: Water sources accessed by arid zone riparian trees in highly saline environments, Australia. *Oecologia*. 156, 43-52, 2008.
- 450 Dawson, T. E. and Ehleringer, J. R.: Streamside trees that do not use stream water. *Nature*. 350, 335-337, 1991.
- Dzikiti, S., Schachtschneider, K., Naiken, V., Gush, M., and Le Maitre, D.: Comparison of water-use by alien invasive pine trees growing in riparian and non-riparian zones in the Western Cape Province, South Africa. *Forest Ecology and Management*. 293, 92-102, 2013.
- Ehleringer, J. R. and Dawson, T. E.: Water-uptake by plants-perspectives from stable isotope composition. *Plant Cell and Environment*. 15, 1073-1082, 1992.
- 455 Evaristo, J., Jasechko, S., and McDonnell, J. J.: Global separation of plant transpiration from groundwater and streamflow. *Nature*. 525, 91-107, 2015.
- Evaristo, J., Kim, M., Haren, J. V., Pangle, L. A., Harman, C. J., Troch, P. A., and McDonnell, J. J.: Characterizing the fluxes and age distribution of soil water, Plant Water and Deep Percolation in a Model Tropical Ecosystem. *Water Resources Research*. 55, 3307-3327, 2019.
- 460 Farquhar, G. D., Ehleringer, J. R., and Hubick, K. T.: Carbon isotope discrimination and photosynthesis. *Annual Review of Plant Physiology and Plant Molecular Biology*. 40, 503-537, 1989.
- Horton, J. L. and Clark, J. L.: Water table decline alters growth and survival of *Salix gooddingii* and *Tamarix chinensis* seedlings. *Forest Ecology and Management*. 140, 239-247, 2001.



- 465 Jasechko, S., Seybold, H., Perrone, D., Fan, Y., and Kirchner, J. W.: Widespread potential loss of streamflow into underlying aquifers across the USA. *Nature*. 591, 391-395, 2021.
- Li, Y., Ma, Y., Song, X. F., Wang, L. X., and Han, D. M.: A $\delta^2\text{H}$ offset correction method for quantifying root water uptake of riparian trees. *Journal of Hydrology*. 593, 125811, doi:10.1016/j.jhydrol.2020.125811, 2021.
- 470 Liu, B., Guan, H. D., Zhao, W. Z., Yang, Y. T., and Li, S. B.: Groundwater facilitated water-use efficiency along a gradient of groundwater depth in arid northwestern China. *Agricultural and Forest Meteorology*. 233, 235-241, 2017.
- Long, D., Yang, W., Scanlon, B. R., Zhao, J., Liu, D., Burek, P., Pan, Y., You, L., and Wada, Y.: South-to-North water diversion stabilizing Beijing's groundwater levels. *Nature Communications*. 11, 3665, doi:10.1038/s41467-020-17428-6, 2020.
- 475 Maxwell, R. M. and Condon, L. E.: Connections between groundwater flow and transpiration partitioning. *Science*. 353, 377-380, 2016.
- Mensforth, L. J., Thorburn, P. J., Tyerman, S. D., and Walker, A. P.: Sources of water used by riparian *Eucalyptus camaldulensis* overlying highly saline groundwater. *Oecologia*. 100, 21-28, 1994.
- 480 Miguez-Macho and G., Fan, Y.: Spatiotemporal origin of soil water taken up by vegetation. *Nature*. 598, 624-628, doi:10.1038/s41586-021-03958-6, 2021.
- Missik, J. E. C., Liu, H. P., Gao, Z. M., Huang, M. Y., Chen, X. Y., Arntzen, E., McFarland, D. P., Ren, H. Y., Titzler, P. S., Thomle, J. N., and Goldman, A.: Groundwater-river water exchange enhances growing season evapotranspiration and carbon uptake in a semiarid riparian ecosystem. *Journal of Geophysical Research-Biogeosciences*. 124, 99-114, 2019.
- 485 Mkunyan, Y. P., Mazvimavi, D., Dziki, S., and Ntshidi, Z.: A comparative assessment of water use by *Acacia longifolia* invasions occurring on hillslopes and riparian zones in the Cape Agulhas region of South Africa. *Physics and Chemistry of the Earth*. 112, 255-264, 2019.
- Moore, G. W. and Owens, M. K.: Transpirational water loss in invaded and restored semiarid riparian forests. *Restoration Ecology*. 20, 346-351, 2012.
- 490 Qian, J., Zheng, H., Wang, P. F., Liao, X. L., Wang, C., Hou, J., Ao, Y., Shen, M. M., Liu, J. J., and Li, K.: Assessing the ecohydrological separation hypothesis and seasonal variations in water use by *Ginkgo biloba*



- L.* in a subtropical riparian area. *Journal of Hydrology*. 553, 486-500, 2017.
- Schindler, D. W. and Donahue, W. F.: An impending water crisis in Canada's western prairie provinces. 495
Proceedings of the National Academy of Sciences of the United States of America. 103, 7210-7216, 2006.
- Smith, K., Liu, S., Hu, H. Y., Dong, X., and Wen, X.: Water and energy recovery: The future of wastewater in
China. *Science of The Total Environment*. 637-638, 1466-1470, 2018.
- Sprenger, M., Llorens, P., Cayuela, C., Gallart, F., and Latron, J.: Mechanisms of consistently disjunct soil water
pools over (pore) space and time. *Hydrology and Earth System Sciences*. 23, 2751-2762, 2019.
- 500 Stellato, L., Terrasi, F., Marzaioli, F., Belli, M., Sansone, U., and Celico, F.: Is ²²²Rn a suitable tracer of stream-
groundwater interactions? A case study in central Italy. *Applied Geochemistry*. 32, 108-117, 2013.
- Stock, B. C. and Semmens, B. X.: MixSIAR GUI User Manual, version 1.0. <http://conserver.iugocafe.org/user/brice.semmens/MixSIAR>, 2013.
- Sun, S. F., Huang, J. H., Han, X. G., and Lin, G. H.: Comparisons in water relations of plants between newly
505 formed riparian and non-riparian habitats along the bank of Three Gorges Reservoir, China. *Trees*. 22, 717-
728, 2008.
- Thorburn, P. J. and Walker, G. R.: Variations in stream water-uptake by *Eucalyptus camaldulensis* with differing
access to stream water. *Oecologia*. 100, 293-301, 1994.
- Wang, J., Fu, B., Lu, N., Wang, S., and Zhang, L.: Water use characteristics of native and exotic shrub species in
510 the semi-arid Loess Plateau using an isotope technique. *Agriculture, Ecosystems & Environment*. 276, 55-
63, 2019b.
- Wang, P. Y., Liu, W. J., Zhang, J. L., Yang, B., Singh, A. K., Wu, J. E., and Jiang, X. J.: Seasonal and spatial
variations of water use among riparian vegetation in tropical monsoon region of SW China. *Ecohydrology*.
12, 14, doi:10.1002/eco.2085, 2019a.
- 515 Wang, Y. S., Yin, D. C., Qi, X. F., and Xu, R. Z.: Hydrogen and oxygen isotopic characteristics of different
water and indicative significance in Baiyangdian Lake. *Environmental Science*. 43, 4,
doi:10.13227/j.hjcx.202108202, 2021. (In chinese).
- White, J. C. and Smith, W. K.: Water source utilization under differing surface flow regimes in the riparian
species *Liquidambar styraciflua*, in the southern Appalachian foothills, USA. *Plant Ecology*. 221, 1069-
520 1082, 2020.



Winter, T. C., Harvey, J. W., Franke, O. L., and Alley, W. M.: Ground water and surface water: A single resource.

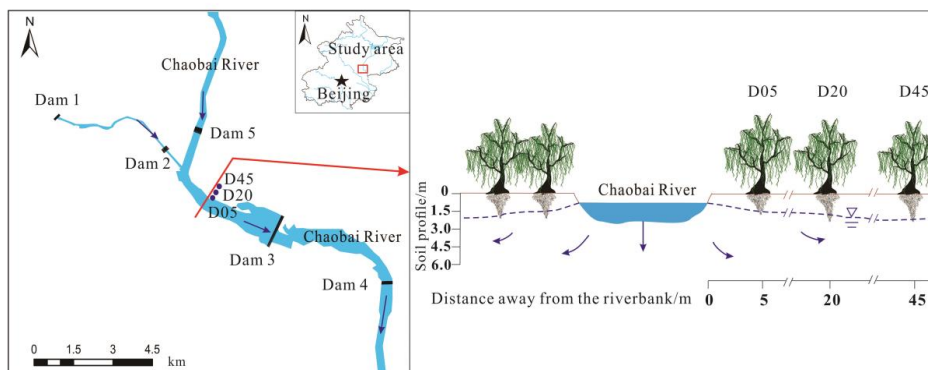
Usgs U.s.geological Survey. 1139, 1998.

Xia, J. B., Ren, J. Y., Zhao, X. M., Zhao, F. J., Yang, H. J., and Liu, J. H.: Threshold effect of the groundwater depth on the photosynthetic efficiency of *Tamarix chinensis* in the Yellow River Delta. *Plant and Soil*. 433,

525 157-171, 2018.

Zhou, T. H., Zhao, C. Y., Wu, G. L., Jiang, S. W., and Yu, Y. X., Wang, D. D.: Application of stable isotopes in analyzing the water sources of *Populus euphratica* and *Tamarix ramosissima* in the upstream of Tarim

river. *Journal of Desert Research*. 37, 124-131, 2017. (in Chinese).



530

Figure 1: Schematic diagram of the study area and the three sampling plots (D05, D20, and D45). D05, D20, and D45 are the plots at distance of 5 m, 20 m, and 45 m away from the riverbank, respectively.

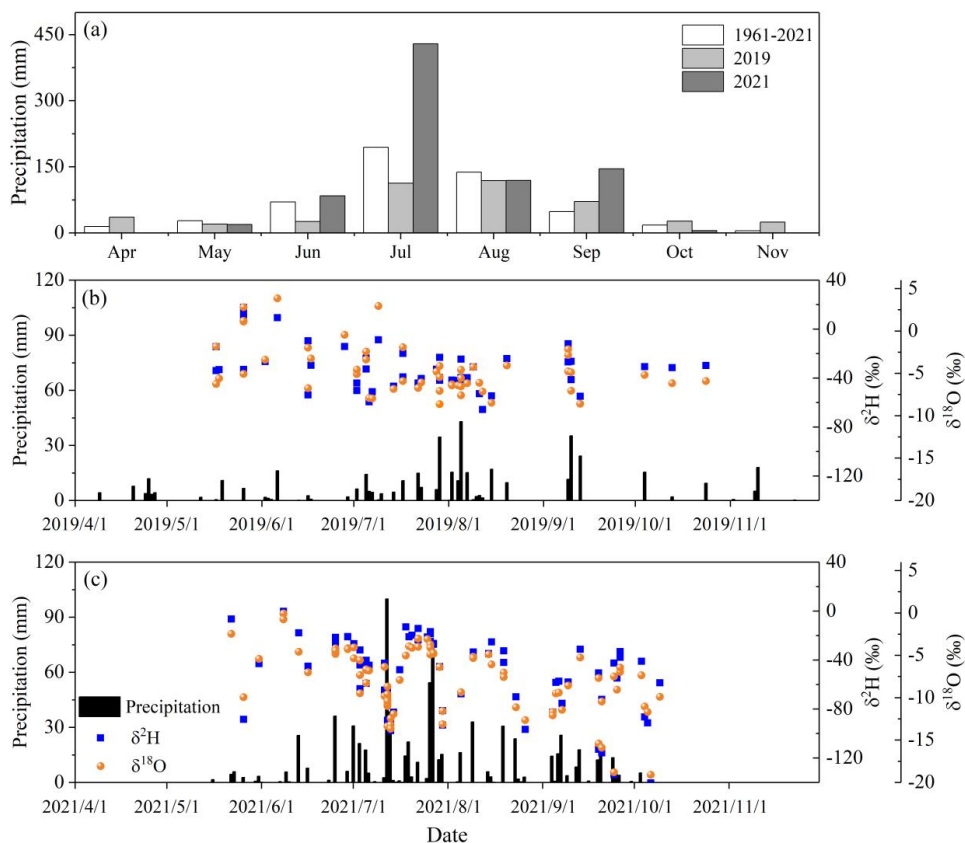
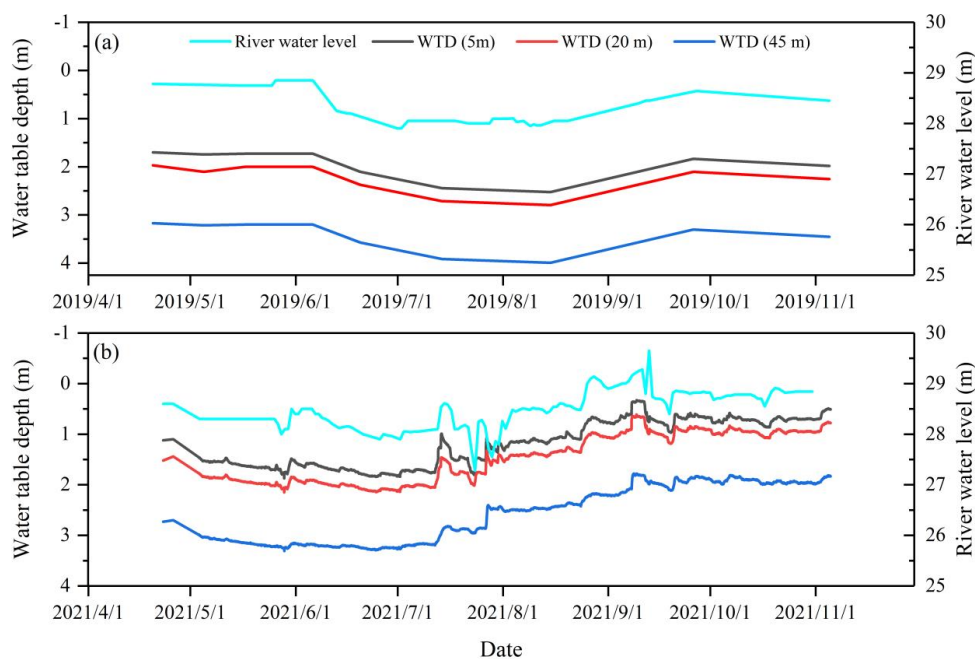
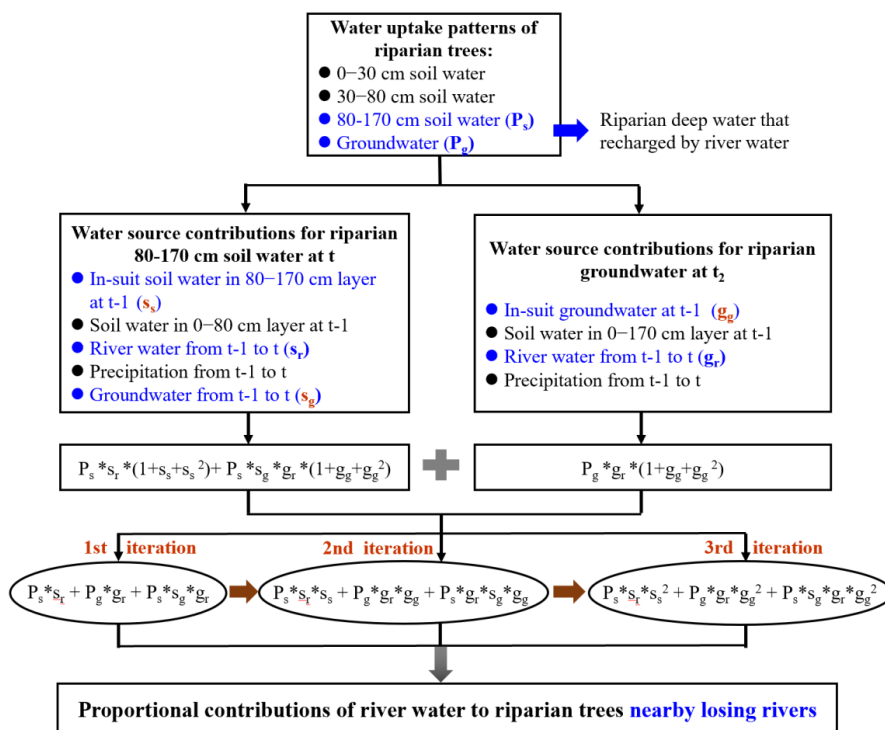


Figure 2: Changes in (a) average monthly precipitation between April and November from 1961 to 2021 and that in the observation years (2019 and 2021), and daily variations in the precipitation and their isotopic compositions in (b) 2019 and (c) 2021.



535

Figure 3: Seasonal variations of the river water level and water table depth (WTD) at distances of 5 m, 20 m, and 45 m away from the riverbank during the observation period in (a) 2019 and (b) 2021.



540 **Figure 4: Flowchart for quantifying the proportional contributions of river water to riparian trees.**

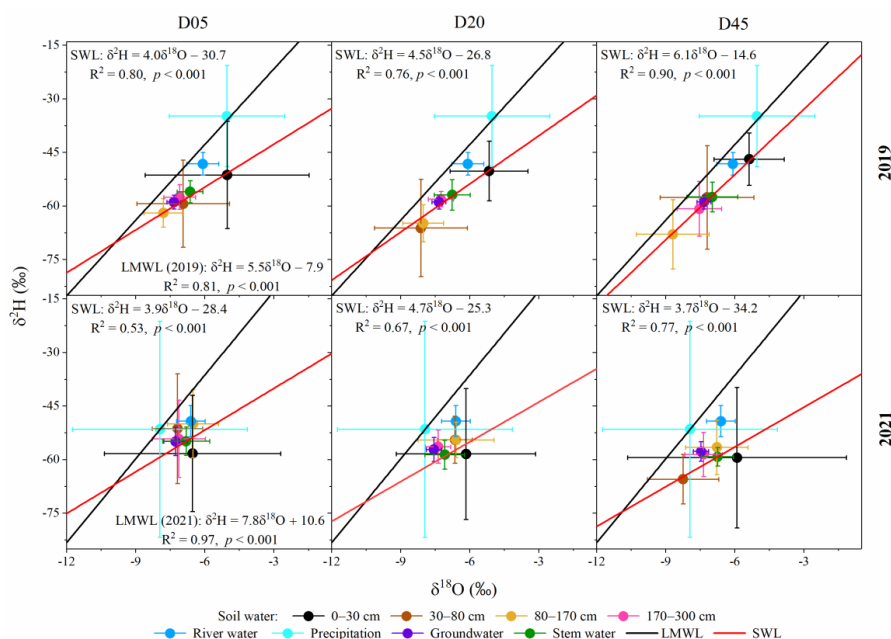


Figure 5: Dual-isotope ($\delta^2\text{H}$ and $\delta^{18}\text{O}$) biplots of different water bodies in three plots (D05, D20, and D45) during the observation period in 2019 and 2021. The Local Meteoric Water Line (LMWL) was fitted by the isotopic values of precipitation in each year. The soil water line (SWL) was fitted by the water isotopes in all soil layers in the three plots (D05, D20, and D45) in each year. D05, D20, and D45 are the plots at distance of 5 m, 20 m, and 45 m away from the riverbank, respectively. The error bars indicate standard deviations.

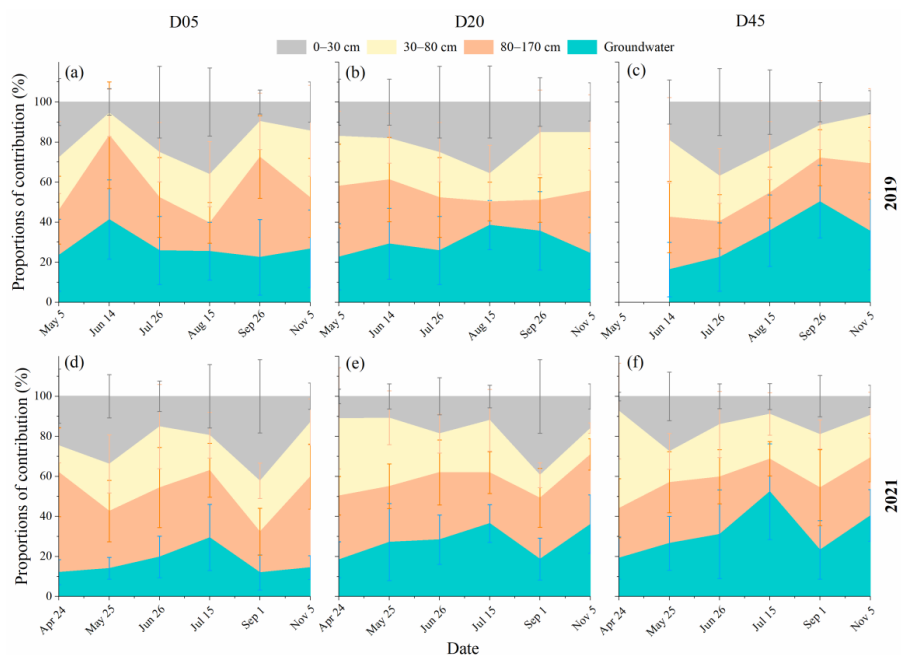


Figure 6: Seasonal water uptake patterns of riparian *S. babylonica* in three plots (D05, D20, and D45) during the observation period in 2019 (a–c) and 2021 (d–f). D05, D20, and D45 are the plots at distance of 5 m, 20 m, and 45 m away from the riverbank, respectively. The error bars indicate standard deviations.

545

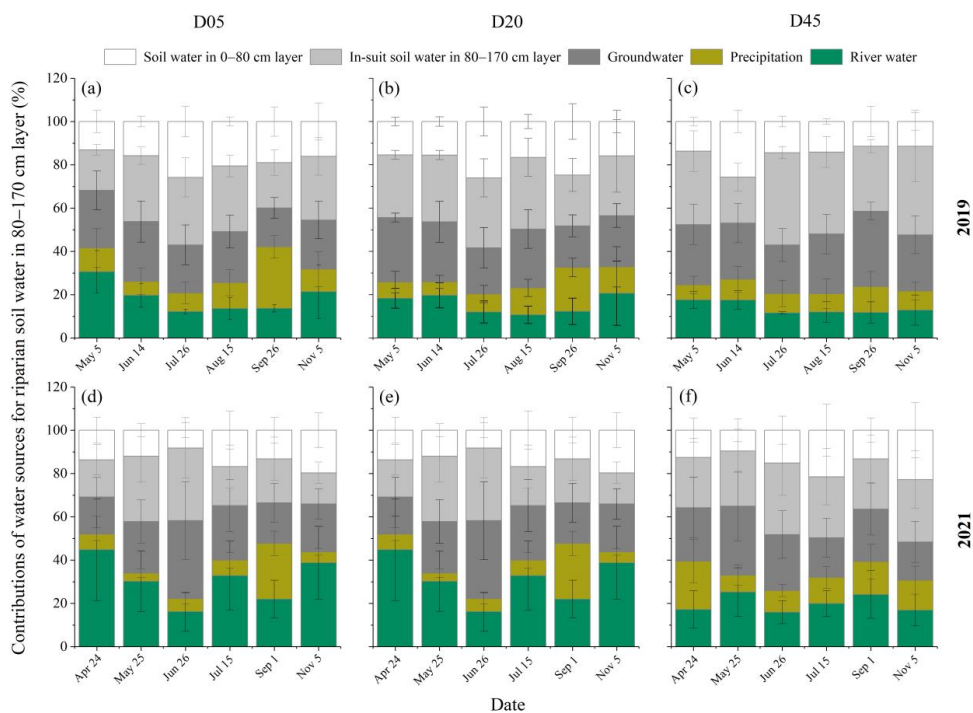
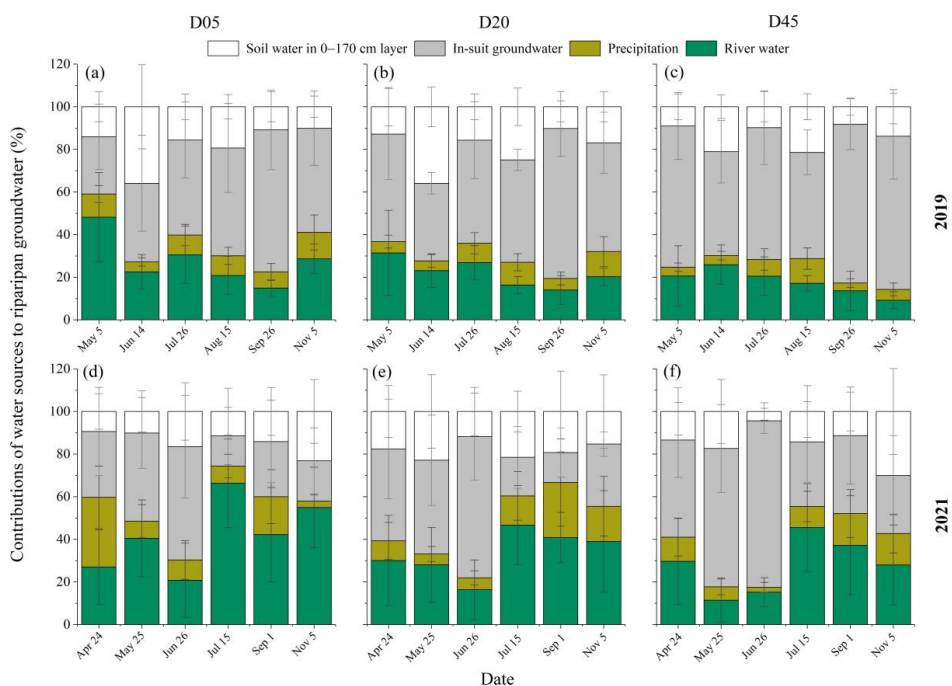


Figure 7: Seasonal variations in the different water source contributions to riparian deep soil water in 80–170 cm layer in three plots (D05, D20, and D45) during the observation period in 2019 (a–c) and 2021 (d–f). D05, D20, and D45 are the plots at distance of 5 m, 20 m, and 45 m away from the riverbank, respectively. The error bars indicate standard deviations.



550

Figure 8: Seasonal variations in the different water source contributions to riparian groundwater in three plots (D05, D20, and D45) during the observation period in 2019 (a–c) and 2021 (d–f). D05, D20, and D45 are the plots at distance of 5 m, 20 m, and 45 m away from the riverbank, respectively. The error bars indicate standard deviations.

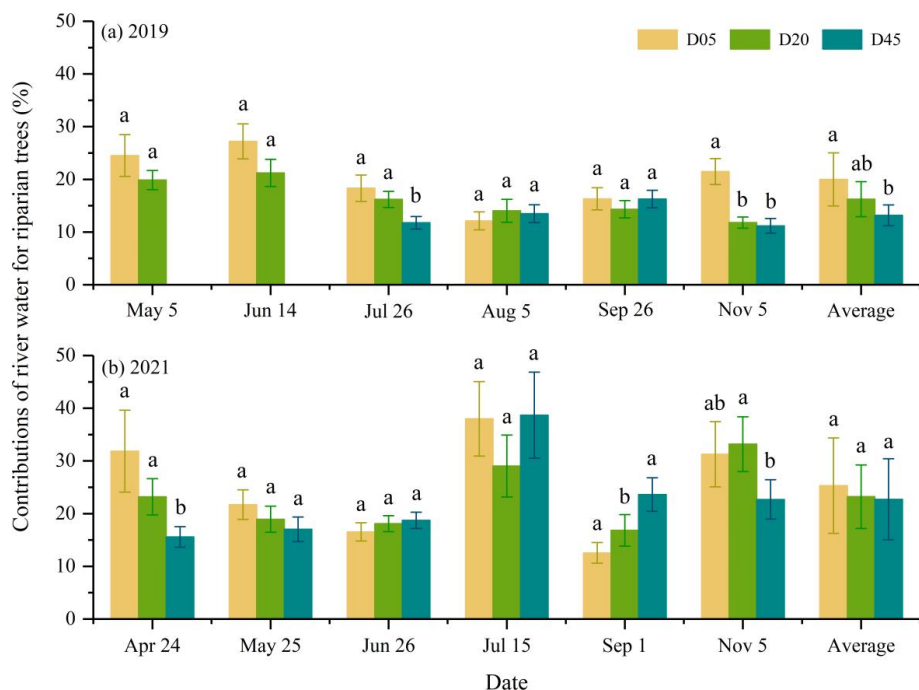


Figure 9: Seasonal variations of the river water contributions to riparian *S. babylonica* in three plots (D05, D20, and D45) during the observation period in (a) 2019 and (b) 2021. The different letters represent significant differences in the river water contributions to riparian *S. babylonica* in the three plots ($p < 0.05$). D05, D20, and D45 are the plots at distance of 5 m, 20 m, and 45 m away from the riverbank, respectively.

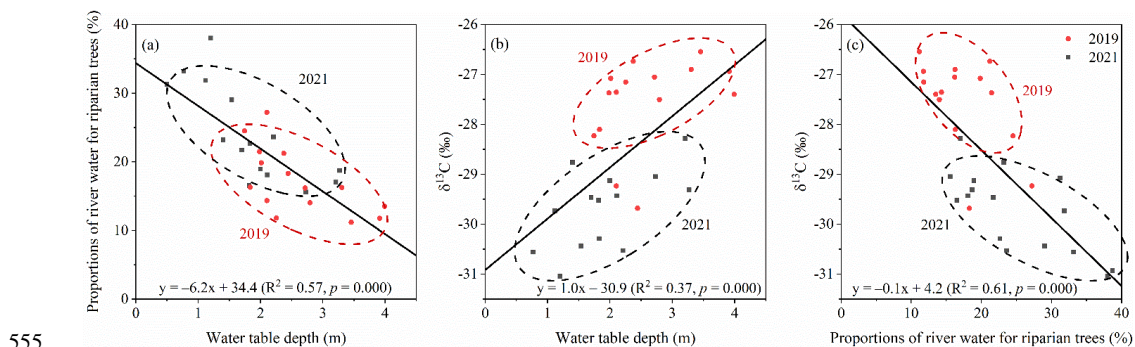


Figure 10: Relationships between (a) the river water contributions to riparian *S. babylonica* and the water table depth, (b) the leaf $\delta^{13}C$ values and the water table depth, and (c) the leaf $\delta^{13}C$ values and river water contributions to riparian *S. babylonica*.



Table 1: Leaf $\delta^{13}\text{C}$ values of riparian *S. babylonica* in three plots (D05, D20, and D45) during the observation period in 2019 and 2021.

	Leaf $\delta^{13}\text{C}$ value (‰)								
	2019							Mean	STD
	May 5	Jun 14	Jul 26	Aug 15	Sep 26	Nov 5			
D05	-28.8	-29.2	-29.7	-30.4	-28.1	-27.4	-28.8	1.0	
D20	-27.1	-26.7	-27.1	-27.5	-27.4	-27.2	-27.1	0.2	
D45	Null	-27.2	-26.9	-27.4	-26.9	-26.5	-27.0	0.3	
	2021							Mean	STD
	Apr 24	May 25	Jun 26	Jul 14	Sep 1	Nov 5			
	D05	-29.7	-29.5	-29.5	-31.0	-29.5	-29.1	-29.7	0.6
D20	-28.8	-29.1	-29.4	-30.4	-30.1	-30.3	-29.7	0.7	
D45	-29.0	-29.0	-29.4	-30.8	-30.1	-30.0	-29.7	0.9	

Note: D05, D20, and D45 are the plots at distance of 5 m, 20 m, and 45 m away from the riverbank, respectively. STD

560 represents standard deviations.



Table 2: The ^{222}Rn values in river water, background groundwater and riparian groundwater in three plots (D05, D20, and D45), and the average residence time of groundwater (T_{res}) in 2021. The background groundwater represents groundwater in aquifers more than 100 m away from the riverbank.

	River water	Background groundwater	Riparian groundwater		
			D05	D20	D45
^{222}Rn value (Bq/m^3)	610.1 ± 212.3	7400	494.5 ± 107.5	763.3 ± 118.3	787.4 ± 153.2
T_{res} (days)	0	Null	-0.09 ± 0.09	0.13 ± 0.1	0.15 ± 0.13

Notes: D05, D20, and D45 are the plots at distance of 5 m, 20 m, and 45 m away from the riverbank, respectively.